Relationship Between Number of Lateral Intercondylar Ridges and Area of Denser Bone on the Lateral Intercondylar Wall

Zijian Li,* MMed, Wentao Zhang,*† MD, Shiyou Ren,* MMed, Ri Zhou,* MD, Xintao Zhang,* MD, Tian You,* MD, and Lu Bai,* MD

Investigation performed at the Department of Sports Medicine and Rehabilitation, Peking University Shenzhen Hospital, Shenzhen, China

Background: A deeper understanding of the anatomy of the intercondylar notch of the femur may help reduce technical errors during anatomic anterior cruciate ligament (ACL) reconstruction.

Purposes: To classify the number of ridges on the lateral intercondylar wall, identify factors influencing the number of ridges, and define the relationship between the area of denser bone on the lateral intercondylar wall and the lateral intercondylar ridge.

Study Design: Descriptive laboratory study.

Methods: Included were 89 patients with computed tomography (CT) images of the knee joint. On full lateral view of the lateral femoral condyle, the authors evaluated for the presence of a lateral intercondylar ridge. The height and area of the lateral intercondylar wall (notch height and lateral notch area) and the length of Blumensaat line were calculated. Notch outlet length, axial notch area, notch width index, and transepicondylar length were also calculated using 3-dimensional CT. Maximum intensity projection was used to identify the area of denser bone on the femoral lateral intercondylar wall, and the relationship between this area and the lateral intercondylar ridge was investigated.

Results: The lateral intercondylar ridge exhibited 3 types of morphological variations. The invisible type (no ridge) was observed in 20 knees (22.5%); the ridge type (1 ridge), in 23 knees (25.8%); and the plateau type (2 ridges), in 46 knees (51.7%). There were significant differences in notch height, lateral notch area, Blumensaat line length, and denser bone area among the ridge types ($P \leq .031$ for all). The locations of the anterior ridge of the plateau type and of all 23 ridges of the ridge type corresponded to the anterior margin line of the area of denser bone.

Conclusion: Significant differences were seen in the 3 types of lateral intercondylar ridges. The anterior margin line of the denser bone area on the lateral intercondylar wall was found to correspond to the anterior border of the plateau type and the ridge type.

Clinical Relevance: The variations in the lateral intercondylar ridge may affect measurement accuracy during evaluation of ACL tunnel position while using the ridge as a landmark. The plateau-type ridge and the area of denser bone on the lateral intercondylar wall may provide a new way for surgeons to determine the femoral tunnel.

Keywords: anatomy; lateral intercondylar ridge; anterior cruciate ligament; attachment site

Over the past several decades, reconstruction of the anterior cruciate ligament (ACL) has been considered the standard for treatment of ACL rupture.[3] In 1996, Laboureau and Marnat-Perrichet[18] placed the graft in the "over-the-top" position close to the proximal aspect of the ACL footprint to minimize the change in ligament length over the normal range of knee motion. Subsequent biomechanical research has shown that the ACL is not isometric and thus needs adequate tension at an appropriate angle during knee motion instead of supporting the same tension at all angles.[5] The anteromedial bundle of the ACL becomes taut at 90° of flexion, and the posterolateral bundle becomes tight as the knee approaches full extension.[4,11,23,36]

As the anatomy and biomechanics of the ACL have become better understood, an anatomic approach to ACL reconstruction has been increasingly applied. However, this has led to a higher graft failure rate, and some patients have developed knee joint dysfunction after incorrect femoral tunnel placement during "anatomic" ACL reconstruction.[13,25,28] Deeper understanding of the anatomy of the intercondylar notch of the femur may help reduce technical errors while performing anatomic ACL reconstruction.

The Orthopaedic Journal of Sports Medicine, 10(5), 23259671221091332
DOI: 10.1177/23259671221091332

The use of the lateral intercondylar ridge as a landmark to guide accurate femoral tunnel placement during anatomic ACL reconstruction is recognized by many surgeons.[1,10,21,34] This ridge is situated three-fourths of the way back on the lateral roof of the intercondylar notch and the lateral intercondylar wall. Iwahashi et al[17] performed histological analyses and identified distinct direct and indirect femoral ACL insertional anatomy. Ferretti et al[9] reported that there is an absence of ACL attachment anterior to the lateral intercondylar ridge. Formation of the lateral intercondylar ridge is thought to occur via the following mechanism: when the bones are loaded in different ways and directions, the bones produce certain stress to counter external stimulus and their morphological structure changes in an adaptive manner, in accordance with Wolff's law.[34] The bones also become denser and thicker in the area corresponding to the functional footprint of the ACL, where they are subjected to a higher level of stress.[30]

Norman et al[22] identified an area with cortical thickening on the lateral wall of the intercondylar notch, which was consistent with the functional ACL footprint. In some patients, the thickened area was located anterior to the lateral intercondylar ridge, which did not match the commonly believed functional footprint of the ACL. We believe that the area with increased bone density is more appropriate for the functional footprint of the ACL.

Ferretti et al[9] showed that the direct fiber of the ACL insertion carries more force than the indirect fiber carries. If this is true, another ridge could form between the direct and indirect femoral ACL insertion from different forces. Only 1 previous study has identified 2 lateral intercondylar ridges on the lateral intercondylar wall among femoral specimens.[31] In that study, 2 ridges were observed in 3.3% of the 299 femurs with a visible lateral intercondylar ridge. However, we have personally observed during arthroscopic surgery that a high proportion of femurs have 2 lateral intercondylar ridges.

The purpose of the current study was to classify the lateral intercondylar ridge according to the number of ridges. We used 3-dimensional (3D) computed tomography (CT), as it can show and allow measurement of the lateral intercondylar ridge.[6] We further aimed to identify factors influencing the morphology of the lateral intercondylar ridge and to define the relationship between the area of denser bone on the lateral intercondylar wall and the lateral intercondylar ridge. The hypothesis was that the number of ridges on the lateral intercondylar notch would vary and that the bone below the femoral ACL insertion would be denser than other areas on the lateral intercondylar notch. We also hypothesized that differences in patient and bony morphological characteristics may lead to differences in the number of ridges.

METHODS

Patient Selection

This study included patients who underwent 3D CT examination of the knee joint at our institution between May 2020 and December 2020. Patients were excluded if they met any of the following criteria: (1) history of ACL rupture and/or previous history of ACL reconstruction, (2) severe osteoarthritis rendering bony landmarks on the lateral intercondylar notch undetectable, or (3) history of fracture to the lateral femoral condyle. Ultimately, 89 patients were enrolled in this study. We obtained 3D CT data and characteristics for all patients.

The experimental protocol was established according to the ethical guidelines of the Helsinki Declaration, and the study was approved by the human ethics committee of Peking University, China. All participants gave written informed consent.

3D CT Imaging

Scanning of all knees was performed at a slice thickness of 0.8 mm using a CT scanner (SOMATOM Definition Flash; Siemens Medical Solutions). The CT data were reconstructed using the RadiAnt DICOM Viewer (Medixant) for image analysis, and reconstruction of the 3D images of the lateral intercondylar wall was performed using CT data using a 3D volume-rendering technique. Based on the method described by Lertwanich et al,[19] the distal femoral model was first placed horizontally in the strictly lateral position, in which superimposition of both femoral condyles was achieved. Then, the model was rotated to a distal view, and the medial femoral condyle was virtually deleted at the highest point of the anterior aperture of the intercondylar notch, leaving behind the lateral femoral condyle. Therefore, a full lateral 3D CT view of the lateral femoral condyle was obtained, and the presence of ridges was evaluated from multiple orientations (Figure 1). Variations in the number of lateral intercondylar ridges were noted and classified.

Femoral Condyle Measurement on 3D CT

On the full lateral 3D CT view of the lateral femoral condyle, we calculated the height and area of the lateral intercondylar wall (notch height and notch area) as well as the

†Address correspondence to Wentao Zhang, MD, Department of Sports Medicine and Rehabilitation, Peking University Shenzhen Hospital, Shenzhen 518036, China (email: zhangwt2007@sina.cn).

*Department of Sports Medicine and Rehabilitation, Peking University Shenzhen Hospital, Shenzhen, China.

Final revision submitted December 17, 2021; accepted February 3, 2022.

The authors declared that they have no conflicts of interest in the authorship and publication of this contribution. AOSSM checks author disclosures against the Open Payments Database (OPD). AOSSM has not conducted an independent investigation on the OPD and disclaims any liability or responsibility relating thereto.

Ethical approval for this study was obtained from Peking University.

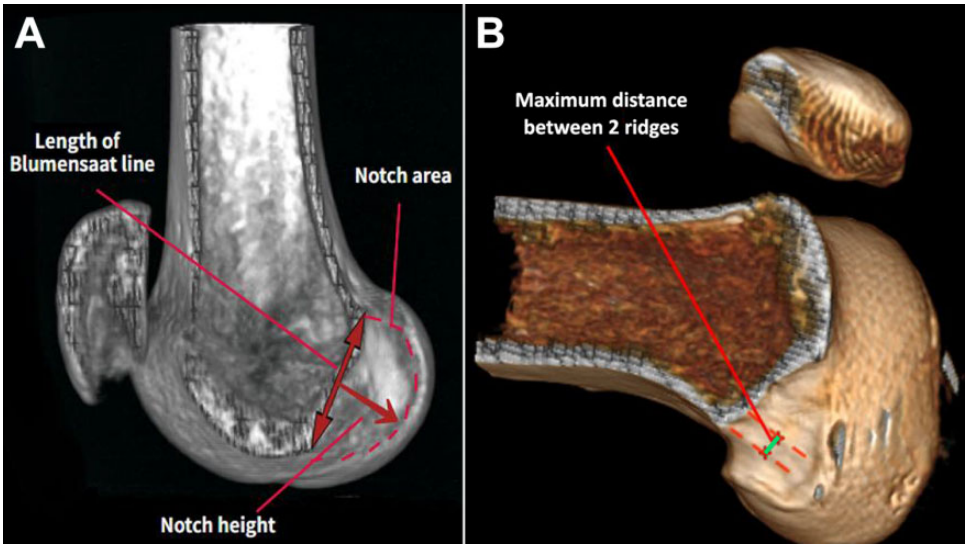

Figure 1. The medial femoral condyle was virtually deleted at the highest point of the anterior aperture of the intercondylar notch to obtain a full lateral 3-dimensional computed tomography view of the lateral femoral condyle. (A) The notch height, notch area, and Blumensaat line length on the lateral wall of the femoral intercondylar notch were outlined and calculated. (B) If 2 ridges were detected, the maximum distance between the ridges (green line) was measured.

length of the Blumensaat line on the lateral wall of the femoral intercondylar notch (Figure 1A). In cases in which 2 lateral intercondylar ridges were identified, the maximum distance between the ridges was measured (Figure 1B). The CT image slice that showed the maximum length between the medial and lateral femoral epicondyles (transepicondylar length [TEL]) was applied. We measured the TEL, notch outlet length, and length of the posterior condyle (Figure 2). The notch width index (NWI) was measured as follows: length of the notch outlet/length of the medial and lateral posterior condyles $\times$ 100%. The axial notch area was assessed using the same slice of the CT image. The notch was delineated, and the posterior border of the notch was determined as the line between the inner aspects of the medial and lateral femoral condyles, which showed a rapid change in slope, as described by Iriuchishima et al.[16] All CT measurements were obtained using a picture archiving and communication system.

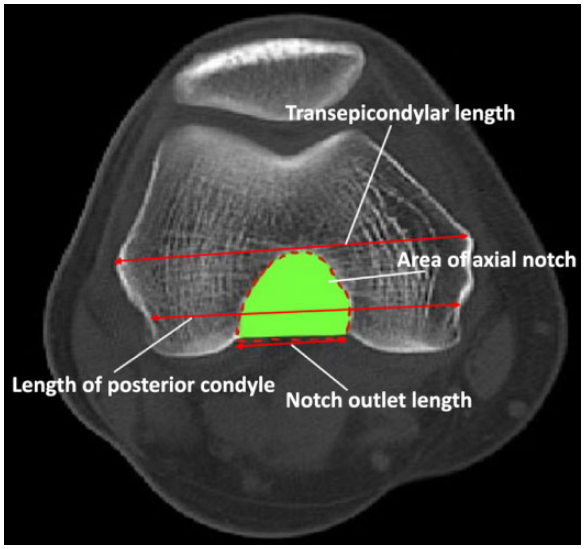

Figure 2. The transepicondylar length, area of the axial notch, notch outlet length, and notch width index (notch outlet length/posterior condylar length) were measured on the same axial slice on the computed tomography image.

Area of Denser Bone on the Lateral Intercondylar Wall

Maximum intensity projection (MIP) was used to obtain a visual representation of the area of denser bone on the lateral intercondylar wall. Reformatting of the MIP images was performed by projecting the voxel having the maximum value in a selected volume of the image onto a 2-dimensional image.[2] We used the "MIP B/W [bones/water] inverse" image setting on the RadiAnt DICOM Viewer to compare differences in bone density (as measured via Hounsfield unit[14] [HU]) in the lateral intercondylar wall. On this setting, the denser bone area is shown as a darker signal.

Farrow et al[7] recommended a standard of 700 HU for accurate cortical bone segmentation in a CT image. Thus, through use of a window width of 400 HU and a level of 700 HU (which starts at 500 HU and enhances to complete darkness at 900 HU), a voxel showing an attenuation value $<$400 HU would be bright and would be allocated 0% bone, a voxel showing an attenuation value of 700 HU would be gray and would be allocated 50% bone ([700–500 HU]/400 HU = 50%), and a voxel showing an attenuation value $\geq$900 HU would be allocated 100% bone. We then measured the dark area on the lateral intercondylar wall, which

Figure 3. Area of denser bone (dashed red line) as observed on the lateral wall of the intercondylar notch on a maximum intensity projection image with "MIP B/W inverse" setting. B/W, bones/water; MIP, maximum intensity projection.

represents the denser bone area (Figure 3). The lateral intercondylar ridges were outlined, and the positional relationship between the ridges was analyzed.

Statistical Analysis

Two authors (Z.L., S.R.) independently performed observations and obtained measurements. The data were measured 3 times, and the average value was considered as the result. If there was a discrepancy in the classification of the intercondylar ridge, the images were evaluated by a third experienced reviewer (W.Z.), and the classification was decided among the 3 researchers.

The study variables included patient characteristics (age, sex, height, and weight), femoral condyle measurements (TEL, notch outlet length, NWI, axial notch area, length of Blumensaat line, notch height, and lateral notch area), and the area of denser bone on the lateral intercondylar wall. For each variable, the mean value was determined and acted as the cutoff for equally dividing the patients into 2 groups, and we utilized chi-square analysis to evaluate the differences in each categorical variable among the intercondylar ridge types. In addition, we used the Pearson correlation coefficient (r) to evaluate the association of the study variables to the maximum distance between 2 lateral intercondylar ridges. Statistical analyses were conducted using SPSS Version 19.0 (IBM Corp). $P < .05$ was considered to indicate statistical significance.

RESULTS

Among the 89 patients included in this study, there were 48 men and 41 women. The mean patient age, height, and weight were 35 ± 16 years, 167 ± 9 cm, and 68 ± 16 kg, respectively.

Morphological Variations in the Lateral Intercondylar Ridge

The lateral intercondylar ridge was identified in 69 of the 89 femurs, whereas invisible ridges were detected in the remaining 20 knees (22.5%) (Figure 4, A-C). Among the 69 femurs with a lateral intercondylar ridge, a single ridge was visible in 23 femurs (33.3%) (Figure 4, D-F), and 2 ridges were identified in 46 femurs (66.7%) (Figure 4, G-I). In cases with 2 lateral intercondylar ridges, a "plateau" could be seen on the lateral intercondylar wall. The lateral intercondylar ridge was thus classified into the following 3 types: invisible, ridge, and plateau.

Femoral Condyle Measurements

The average TEL, NWI, notch outlet length, and axial notch area were 78.4 ± 6.4 mm, 30.1% ± 3.8%, 20.2 ± 3.1 mm, and 230 ± 47.8 mm^2, respectively. The notch height, lateral notch area, and Blumensaat line length were 16.2 ± 2.0 mm, 320.4 ± 73.1 mm^2, and 26.9 ± 2.4 mm, respectively. In the plateau-type lateral intercondylar ridge, the mean maximum distance between the 2 ridges was 4.5 ± 0.5 mm.

Relationship of Lateral Intercondylar Ridge to Area of Denser Bone

In 87 of the 89 femoral samples (97.8%), a dark, ellipse-shaped area could be fitted onto the denser bone area of the lateral intercondylar wall. The mean area of denser bone on the lateral intercondylar wall was 77.41 ± 28.6 mm^2. Among all 46 lateral intercondylar ridges of the plateau type (100%), the anterior ridge of the lateral intercondylar ridge matched the anterior margin line of the denser bone area; however, the relationship of the denser bone area with the posterior ridge of the lateral intercondylar plateau was variable (Figure 5, A and B). All 23 ridges of the ridge-type matched the anterior margin line of the denser bone area (Figure 5C).

Lateral Intercondylar Ridge Types According to Study Variables

There were no significant differences among the ridge types according to patient characteristics. Regarding femoral condyle characteristics, significant differences were seen in Blumensaat line length, notch height, and lateral notch area ($P = .031$, .005, and .003, respectively). Significant differences by ridge type were also seen in the area of denser bone ($P = .008$) (Table 1).

Association of Maximum Distance Between Ridges With Patient and Femoral Condylar Characteristics

The maximum distance between 2 lateral condylar ridges was significantly negatively correlated with patient age

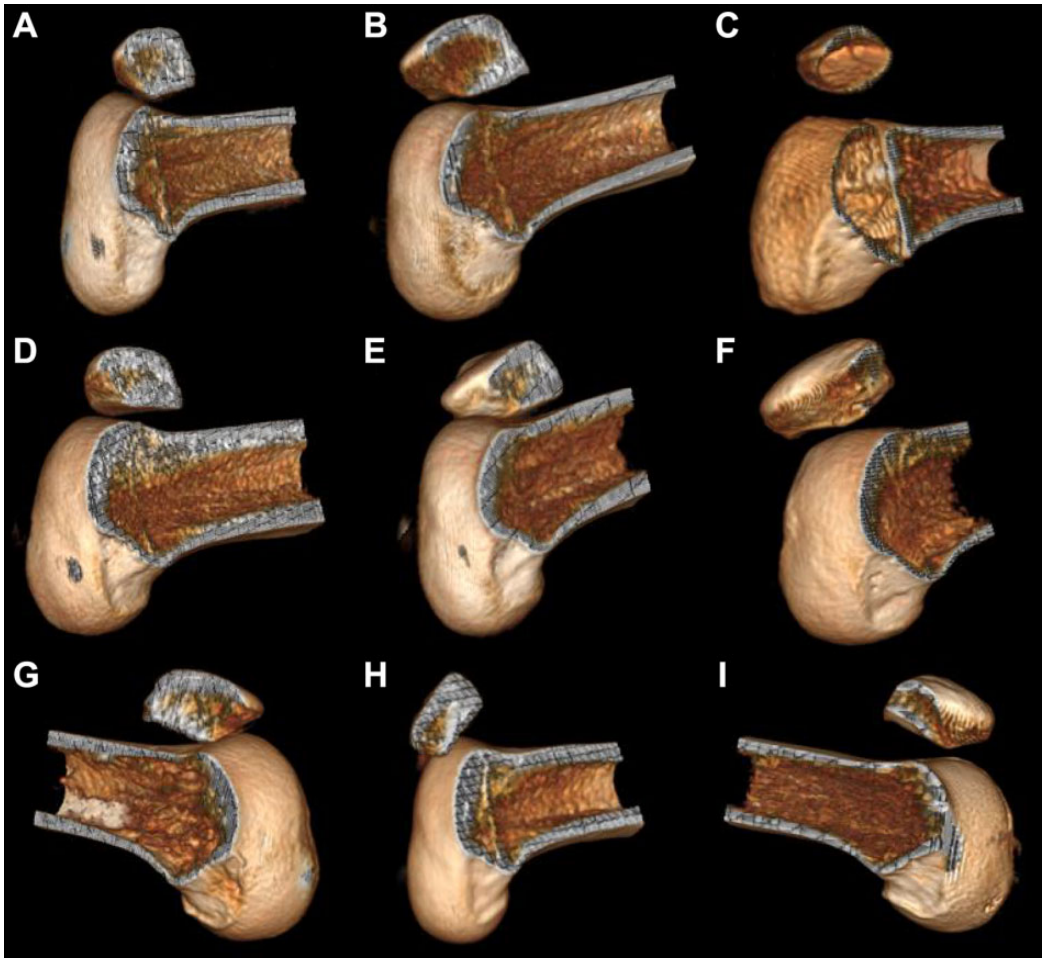

Figure 4. The lateral intercondylar ridge as seen on 3-dimensional computed tomography images was classified into the following 3 types: (A-C) invisible, (D-F) ridge, and (G-I) plateau.

($r = –0.337$; $P = .022$) and significantly positively correlated with area of the lateral intercondylar wall ($r = 0.364$; $P = .013$). The other variables were not significantly correlated with maximum distance between ridges (Table 2 and Figure 6).

DISCUSSION

The main finding noted in this study was that the lateral intercondylar ridge morphology and the number of ridges exhibited variations. In 46 of the 89 femurs (51.7%), we identified 2 ridges with a plateau between them. A second finding was that the lateral notch area, notch height, and Blumensaat line length were significantly different among lateral intercondylar ridge types. The presence of such variations may affect measurement accuracy during evaluation of ACL tunnel position while using the lateral intercondylar ridge as a landmark during anatomic ACL reconstruction. A final finding was that an area of denser bone was formed on the lateral intercondylar wall in 87 of 89 femurs (97.8%). The anterior ridge on the plateau type and the ridge seen on the ridge type were located on the anterior margin of the denser bone area.

Currently, many surgical techniques are used to achieve an ideal anatomical femoral tunnel position. The "clockface" reference has been used to refer to the coronal position of the site of insertion of the ACL and placement of the graft.[20,24,26] However, the position of the clockface is strongly influenced when there is knee movement from extension to flexion, and a 2-dimensional template may not be appropriate for orientation in the shallow-deep direction.[12,35] The other guiding technique works via the femoral ACL remnants, but the femoral ACL remnants are not likely to be visible in chronic cases. Furthermore, the center of the femoral remnants is not a useful center for the femoral footprint.[32] Therefore, the lateral intercondylar ridge is still one of the best options to locate the femoral tunnel.

Many studies have been conducted regarding the lateral intercondylar ridge. Hutchinson and Ash[15] performed an anatomic study and found a distinctive ridge in 9 of the 10 human cadaveric specimens and a change in slope situated approximately 75% posteriorly on the roof and lateral wall of the intercondylar notch of the knee. Farrow et al[7]

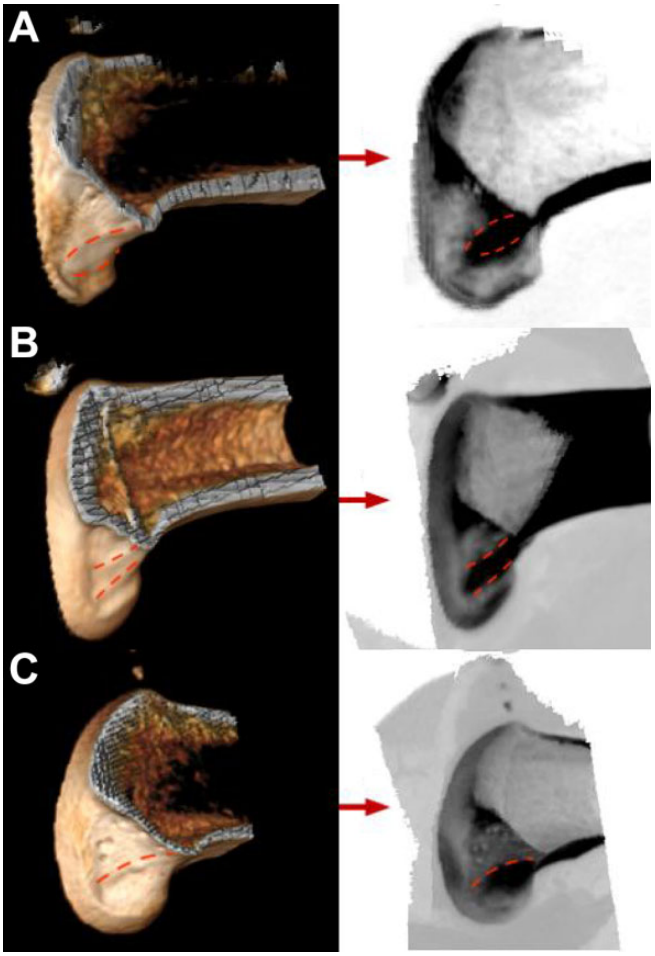

Figure 5. Relationship between the location of the lateral intercondylar ridges (dashed red lines) on 3-dimensional computed tomography images (left) and the area of denser bone on maximum intensity projection images (right). For plateau-type lateral intercondylar ridges, the anterior ridge corresponded to the anterior margin line of the denser bone area, but the relationship between the posterior ridge and denser bone area was variable: the posterior ridge was located either (A) anterior or (B) posterior to the posterior margin line of the denser bone area. (C) All 23 lateral intercondylar ridges of the ridge type corresponded to an anterior margin line of the denser bone area.

TABLE 1
Comparison of Lateral Intercondylar Ridge Types by Patient and Femoral Condylar Characteristics (N = 89)[a]

	Intercondylar Ridge Type			
Variable[b]	Invisible (n = 20)	Ridge (n = 23)	Plateau (n = 46)	*P*
Age (35 ± 16 y)				.079
≤35 y	15	9	28	
>35 y	5	14	18	
Weight (68 ± 16 kg)				.755
≤68 kg	12	13	22	
>68 kg	8	10	24	
Height (167 ± 9.0 cm)				.471
≤167 cm	13	13	22	
>167 cm	7	10	24	
TEL (78.4 ± 6.4 mm)				.249
≤78 mm	8	14	19	
>78 mm	12	9	27	
Notch outlet length (20.2 ± 3.1 mm)				.373
≤20.2 mm	8	9	26	
>20.2 mm	12	14	20	
NWI (30.1% ± 3.8%)				.192
≤30.1%	9	9	28	
>30.1%	11	14	18	
Axial notch area (230 ± 47.8 mm^2)				.943
≤230 mm^2	9	11	20	
>230 mm^2	11	12	26	
Blumensaat line length (26.9 ± 2.4 mm)				.031
≤26.9 mm	15	13	17	
>26.9 mm	5	10	29	
Notch height (16.2 ± 2.0 mm)				.005
≤16.2 mm	16	12	15	
>16.2 mm	4	11	31	
Lateral notch area (320.4 ± 73.1 mm^2)				.003
≤320.4 mm^2	15	15	15	
>320.4 mm^2	5	8	31	
Area of denser bone (77.41 ± 28.6 mm^2)				.008
≤77.41 mm^2	16	8	21	
>77.41 mm^2	4	15	25	

[a]Values are presented as No. NWI, notch width index; TEL, transepicondylar length.
[b]Data in parentheses indicate mean ± SD.

studied 200 human femoral specimens and found the resident's ridge (renamed the lateral intercondylar ridge) in 194 femoral specimens. The authors classified the lateral intercondylar ridge into 2 types: (1) defined and (2) smooth. Tsukada et al,[31] in a cadaveric study, reported large positional and dimensional variations in the lateral intercondylar ridge; the lateral intercondylar ridge was found in 94.0% of 348 human femoral specimens. Iriuchishima et al[16] reported that 29 of 34 cadaveric knees showed the presence of a lateral intercondylar ridge, and the ridge was located at 61.8% ± 4.6% from the posterior condylar line. The lateral intercondylar ridge runs from a point defined by multiplying Blumensaat line length by 0.79 at a 75.5° angle with regard to Blumensaat line, as described by Farrow et al.[8] van Eck et al[34] found that there was no difference in the presence of the lateral intercondylar ridge between patients with acute and chronic ACL injuries. In our study, we classified the morphology of the lateral intercondylar ridge into the following 3 types: (1) invisible, (2) ridge, and (3) plateau. The incidence of the lateral intercondylar ridge in our study population was 77.5%, which was close to that in the above-mentioned studies.

On the basis of our study results, we believe that the plateau type of lateral intercondylar ridge can represent the direct femoral ACL insertion. According to Sasaki

et al,[27] the width of the direct insertion is 5.3 ± 1.1 mm. In this study, the maximum distance between the 2 ridges of the plateau type was 4.5 ± 0.5 mm. These values are relatively close. The lateral intercondylar ridge has been found to correspond with the anterior margin line of the direct femoral ACL insertion.[9,15,17] Suruga et al[29] performed a cadaveric study and noted that the area of the axial notch and length of the notch outlet showed a significant correlation with the area of direct insertion. In a cadaveric study by van Eck et al,[33] the size and shape of the femoral intercondylar notch were correlated with the ACL size. Iriuchishima et al[16] reported that large knees possessed large ACLs. In our study, age was significantly negatively correlated and lateral notch area was significantly positively correlated with the maximum distance between the ridges. However, we found that younger patients had a larger lateral notch area. Therefore, the maximum distance of the lateral intercondylar ridge of the plateau type could only be related to the lateral notch area.

TABLE 2
Association of Maximum Distance Between Ridges of the Plateau Type (n = 46) With Patient and Femoral Condylar Characteristics[a]

Characteristic	*r*	*P*
Age	–0.337	.022
Weight	0.018	NS
Height	0.202	NS
TEL	0.128	NS
Notch outlet length	0.121	NS
NWI	0.118	NS
Axial notch area	0.191	NS
Blumensaat line length	0.013	NS
Notch height	0.124	NS
Lateral notch area	0.364	.013
Area of denser bone	0.027	NS

[a]NS, not significant; NWI, notch width index; TEL, transepicondylar length.

Successful femoral tunnel localization is the key to ACL reconstruction. Ideal knee mechanics are reestablished by placement of the graft inside the anatomical ACL footprint. We observed that patients who had a larger lateral notch area, notch height, Blumensaat line length, and denser bone area were more likely to have the plateau-type lateral intercondylar ridge. Thus, for patients with the plateau-type variation, the use of the posterior ridge as the leading edge of the tunnel may result in a more backward tunnel position. We speculate that the placement of the tunnel in the center of the 2 ridges would be a better option.

This is the first study to identify an area of denser bone on the lateral intercondylar wall at a frequency of 97.8%, which is higher than that of the appearance of a lateral intercondylar ridge (77.5%). We found that the anterior ridge of the plateau type and the single ridge of the ridge type are located on the anterior margin of the denser bone area. In the invisible type of lateral intercondylar ridge, we may be able to use the anterior margin of the denser bone area as the anterior margin line of direct femoral insertion of the ACL. We believe that this area is consistent with that in recent studies,[22] indicating that it represents the functional footprint of the ACL. However, this hypothesis needs further investigation. To verify whether this association is feasible, we plan to analyze the relationship between the reduction ratio of the denser bone area after ACL reconstruction and successful clinical outcomes.

Limitations

The major limitations of this study are as follows. (1) Cadaveric specimens were not included in this study; thus, the lateral intercondylar ridge type could not be observed directly. (2) The accuracy of CT in measuring the maximum distance between the 2 ridges of the plateau type may be lower than that of micro-CT. (3) Only Chinese patients were enrolled in this study; therefore, ethnicity may be an influencing factor and should be considered in further studies.

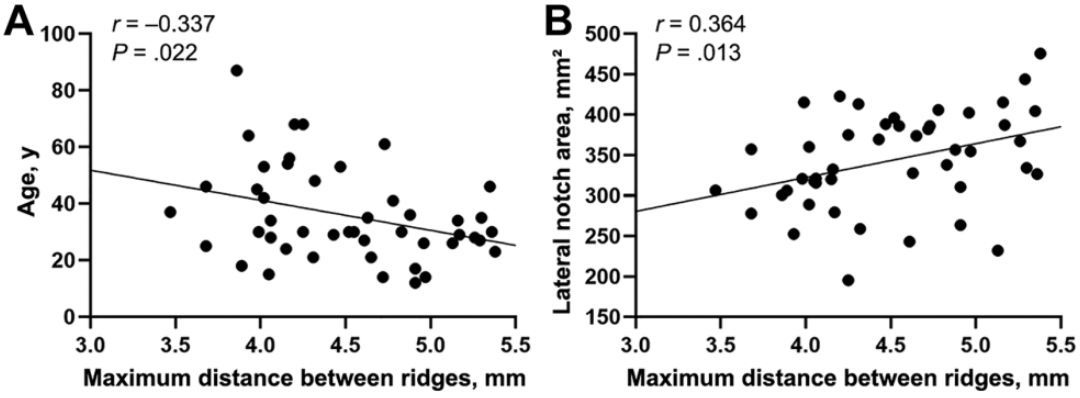

Figure 6. Scatterplot showing significant association of maximum distance between ridges with (A) age and (B) lateral notch area.

CONCLUSION

In this study, we identified the following 3 types of lateral intercondylar ridge via CT scans: invisible, ridge, and plateau. The lateral notch area, notch height, and Blumensaat line length were significantly different among lateral intercondylar ridge types. We also identified a denser bone area on the lateral intercondylar wall, and the anterior margin conformed to the anterior ridge of the plateau type and the ridge type. This study improves our understanding of the bony landmarks on the lateral intercondylar wall and the bony morphology of the lateral intercondylar notch, which may help improve the anatomic ACL reconstruction technique.

REFERENCES

1. Bhattacharyya R, Ker A, Fogg Q, Spencer SJ, Joseph J. Lateral intercondylar ridge: is it a reliable landmark for femoral ACL insertion? An anatomical study. *Int J Surg*. 2018;50:55-59.
2. Calhoun PS, Kuszyk BS, Heath DG, Carley JC, Fishman EK. Three-dimensional volume rendering of spiral CT data: theory and method. *Radiographics*. 1999;19(3):745-764.
3. Chambat P, Guier C, Sonnery-Cottet B, Fayard JM, Thaunat M. The evolution of ACL reconstruction over the last fifty years. *Int Orthop*. 2013;37(2):181-186.
4. Chhabra A, Starman JS, Ferretti M, Vidal AF, Zantop T, Fu FH. Anatomic, radiographic, biomechanical, and kinematic evaluation of the anterior cruciate ligament and its two functional bundles. *J Bone Joint Surg Am*. 2006;88(suppl 4):2-10.
5. Dabirrahmani D, Hogg MC, Walker P, Biggs D, Gillies RM. Comparison of isometric and anatomical graft placement in synthetic ACL reconstructions: a pilot study. *Comput Biol Med*. 2013;43(12):2287-2296.
6. Das A, Yadav CS, Gamanagatti S, Pandey RM, Mittal R. Arthroscopic and 3D CT scan evaluation of femoral footprint of the anterior cruciate ligament in chronic ACL deficient knees. *J Knee Surg*. 2019;32(6):584-588.
7. Farrow LD, Chen MR, Cooperman DR, Victoroff BN, Goodfellow DB. Morphology of the femoral intercondylar notch. *J Bone Joint Surg Am*. 2007;89(10):2150-2155.
8. Farrow LD, Gillespie RJ, Victoroff BN, Cooperman DR. Radiographic location of the lateral intercondylar ridge: its relationship to Blumensaat's line. *Am J Sports Med*. 2008;36(10):2002-2006.
9. Ferretti M, Ekdahl M, Shen W, Fu FH. Osseous landmarks of the femoral attachment of the anterior cruciate ligament: an anatomic study. *Arthroscopy*. 2007;23(11):1218-1225.
10. Fu FH, Jordan SS. The lateral intercondylar ridge—a key to anatomic anterior cruciate ligament reconstruction. *J Bone Joint Surg Am*. 2007;89(10):2103-2104.
11. Hefzy MS, Grood ES, Noyes FR. Factors affecting the region of most isometric femoral attachments, part II: the anterior cruciate ligament. *Am J Sports Med*. 1989;17(2):208-216.
12. Hoshino Y, Kim D, Fu FH. Three-dimensional anatomic evaluation of the anterior cruciate ligament for planning reconstruction. *Anat Res Int*. 2012;2012:569704.
13. Hosseini A, Lodhia P, Van de Velde S, et al. Tunnel position and graft orientation in failed anterior cruciate ligament reconstruction: a clinical and imaging analysis. *Int Orthop*. 2012;36(4):845-852.
14. Hounsfield GN. Nobel Award address: computed medical imaging. *Med Phys*. 1980;7(4):283-290.
15. Hutchinson MR, Ash SA. Resident's ridge: assessing the cortical thickness of the lateral wall and roof of the intercondylar notch. *Arthroscopy*. 2003;19(9):931-935.
16. Iriuchishima T, Goto B, Okano T, Ryu K, Fu FH. Femoral tunnel length in anatomical single-bundle ACL reconstruction is correlated with height, weight, and knee bony morphology. *Knee Surg Sports Traumatol Arthrosc*. 2019;27(1):93-99.
17. Iwahashi T, Shino K, Nakata K, et al. Direct anterior cruciate ligament insertion to the femur assessed by histology and 3-dimensional volume-rendered computed tomography. *Arthroscopy*. 2010;26(9)(suppl):S13-S20.
18. Laboureau JP, Marnat-Perrichet F. Isometric reconstruction of the anterior cruciate ligament: determination of the femoral and tibial tunnels. Article in French. *Acta Orthopaedica Belgica*. 1996;62(suppl 1):166-177.
19. Lertwanich P, Martins CA, Asai S, Ingham SJ, Smolinski P, Fu FH. Anterior cruciate ligament tunnel position measurement reliability on 3-dimensional reconstructed computed tomography. *Arthroscopy*. 2011;27(3):391-398.
20. Loh JC, Fukuda Y, Tsuda E, Steadman RJ, Fu FH, Woo SL. Knee stability and graft function following anterior cruciate ligament reconstruction: comparison between 11 o'clock and 10 o'clock femoral tunnel placement. 2002 Richard O'Connor Award paper. *Arthroscopy*. 2003;19(3):297-304.
21. Nawabi DH, Tucker S, Schafer KA, et al. ACL fibers near the lateral intercondylar ridge are the most load bearing during stability examinations and isometric through passive flexion. *Am J Sports Med*. 2016;44(10):2563-2571.
22. Norman D, Metcalfe AJ, Barlow T, et al. Cortical bony thickening of the lateral intercondylar wall: the functional attachment of the anterior cruciate ligament. *Am J Sports Med*. 2017;45(2):394-402.
23. Papannagari R, Gill TJ, Defrate LE, Moses JM, Petruska AJ, Li G. In vivo kinematics of the knee after anterior cruciate ligament reconstruction: a clinical and functional evaluation. *Am J Sports Med*. 2006;34(12):2006-2012.
24. Raffo CS, Pizzarello P, Richmond JC, Pathare N. A reproducible landmark for the tibial tunnel origin in anterior cruciate ligament reconstruction: avoiding a vertical graft in the coronal plane. *Arthroscopy*. 2008;24(7):843-845.
25. Rothrauff B, Jorge A, de Sa D, Kay J, Fu F, Musahl V. Anatomic ACL reconstruction reduces risk of post-traumatic osteoarthritis: a systematic review with minimum 10-year follow-up. *Knee Surg Sports Traumatol Arthrosc*. 2020;28(4):1072-1084.
26. Rue JP, Ghodadra N, Bach BR Jr. Femoral tunnel placement in single-bundle anterior cruciate ligament reconstruction: a cadaveric study relating transtibial lateralized femoral tunnel position to the anteromedial and posterolateral bundle femoral origins of the anterior cruciate ligament. *Am J Sports Med*. 2008;36(1):73-79.
27. Sasaki N, Ishibashi Y, Tsuda E, et al. The femoral insertion of the anterior cruciate ligament: discrepancy between macroscopic and histological observations. *Arthroscopy*. 2012;28(8):1135-1146.
28. Seijas R, Ares O, Sallent A, Alvarez P, Cusco X, Cugat R. Return to prelesional Tegner level after anatomic anterior cruciate ligament reconstruction. *Arch Orthop Trauma Surg*. 2016;136(12):1695-1699.
29. Suruga M, Horaguchi T, Iriuchishima T, et al. Morphological size evaluation of the mid-substance insertion areas and the fan-like extension fibers in the femoral ACL footprint. *Arch Orthop Trauma Surg*. 2017;137(8):1107-1113.
30. Taylor RE, Zheng C, Jackson RP, et al. The phenomenon of twisted growth: humeral torsion in dominant arms of high performance tennis players. *Comput Methods Biomech Biomed Eng*. 2009;12(1):83-93.
31. Tsukada S, Fujishiro H, Watanabe K, et al. Anatomic variations of the lateral intercondylar ridge: relationship to the anterior margin of the anterior cruciate ligament. *Am J Sports Med*. 2014;42(5):1110-1117.
32. van Eck CF, Lesniak BP, Schreiber VM, Fu FH. Anatomic single- and double-bundle anterior cruciate ligament reconstruction flowchart. *Arthroscopy*. 2010;26(2):258-268.
33. van Eck CF, Martins CA, Vyas SM, Celentano U, van Dijk CN, Fu FH. Femoral intercondylar notch shape and dimensions in ACL-injured patients. *Knee Surg Sports Traumatol Arthrosc*. 2010;18(9):1257-1262.

34. van Eck CF, Morse KR, Lesniak BP, et al. Does the lateral intercondylar ridge disappear in ACL deficient patients? *Knee Surg Sports Traumatol Arthrosc*. 2010;18(9):1184-1188.
35. Wittstein JR, Garrett WE. Time to get rid of the clock: intraobserver and interobserver reliability in determination of the o'clock position of the femoral tunnel in ACL reconstruction. *J Knee Surg*. 2014;27(1): 89-92.
36. Woo LY, Wu C, Dede O, Vercillo F, Noorani AS. Biomechanics and anterior cruciate ligament reconstruction. *J Orthop Surg Res*. 2006;1(1):2.